

OBSERVATIONS OF DIFFUSE INTERSTELLAR BANDS¹ ATTRIBUTED TO C_7^-

B. J. MCCALL, D. G. YORK, AND T. OKA

Department of Astronomy and Astrophysics and the Enrico Fermi Institute, University of Chicago, 5735 South Ellis Avenue, Chicago, IL 60637;
bjmccall@uchicago.edu

Received 1999 July 26; accepted 1999 October 15

ABSTRACT

Recent advances in laboratory gas-phase spectroscopy of large molecules and their ions permit a direct comparison between the diffuse interstellar bands (DIBs) and proposed carriers. On the basis of gas-phase data, Tulej et al. recently suggested that five $A^2\Pi_u \leftarrow X^2\Pi_g$ electronic transitions of the linear carbon-chain anion C_7^- match with DIBs. We have obtained high-resolution visible spectra of four reddened stars (HD 46711, HD 50064, HD 183143, and Cyg OB2 12) to make a detailed comparison with the C_7^- laboratory data. Our data show that three of the C_7^- bands (0_0^0 at 6270.2 Å, 3_0^1 at 6064.0 Å, and $1_0^2 3_0^1$ at 4963.0 Å) are in good agreement with DIBs in wavelength and relative intensity. A fourth band (1_0^1 at 5612.8 Å) also agrees in intensity but is apparently off by 2 Å in wavelength. All other laboratory bands of C_7^- are not expected to be detectable in astronomical spectra with the current level of sensitivity. The gas-phase spectrum of C_7^- agrees with the DIBs better than that of any previously proposed molecule. However, the question of whether C_7^- is a DIB carrier cannot be definitively answered until (1) better laboratory measurements confirm, refute, or explain the wavelength discrepancy for the 1_0^1 band and/or (2) better astronomical spectra reveal the presence or absence of other C_7^- bands.

Subject headings: ISM: molecules — line: identification — methods: laboratory — molecular data

1. INTRODUCTION

The diffuse interstellar bands, a series of absorption features in the visible spectra of reddened stars, have defied explanation for over half a century. It is now generally accepted that the diffuse interstellar bands (DIBs) are most likely due to free molecules in the gas phase (Herbig 1995), but so far there has been no definitive match between a subset of the diffuse bands and the gas-phase spectrum of any individual molecule.

One class of molecules that has been proposed to explain the diffuse bands is carbon-chain molecules. As pointed out by Douglas (1977) and Smith, Snow, & York (1977), rapid internal conversion of electronic energy into vibrational energy in these molecules can explain the “diffuse” character of their spectral lines and also protect the molecules from photodissociation caused by ultraviolet radiation from stars. This explanation has the advantage that diffuse-band carriers need not be destroyed by the absorption (unlike the case of predissociation broadening) and thus do not require replacement by some rapid chemical process. Carbon-chain molecules are also attractive because of the high cosmic abundance of carbon and because they are similar to molecules observed by radio astronomers in dense clouds, such as the cyanopolyacetylenes (Avery et al. 1976). The production and chemical stability of carbon-chain molecules (particularly C_7^-) has been recently examined by Ruffle et al. (1999).

To test potential diffuse-band carriers effectively, gas-phase laboratory spectra are essential. Spectra recorded in rare-gas matrices are far easier to obtain but are subject to unpredictable wavelength shifts that make comparison with astronomical spectra impractical. It has recently become possible, using the technique of resonance-enhanced two-

color photodetachment, to obtain relatively sharp gas-phase spectra of carbon-chain anions. Based on such spectra, Tulej et al. (1998) pointed out that five spectral lines of the C_7^- anion coincide (within 2 Å) with diffuse bands tabulated by Jenniskens & Désert (1994).

Because most of the diffuse bands attributed to C_7^- had a low signal-to-noise ratio in the data of Jenniskens & Désert (1994), it was necessary to improve the astronomical measurements to test the assignment of these lines to C_7^- .

2. OBSERVATIONS AND DATA REDUCTION

High-resolution visible spectra of four reddened and two unreddened stars were obtained using the Astrophysical Research Consortium Echelle Spectrometer (ARCES). ARCES was commissioned from 1999 January to March and is now in routine use on the 3.5 m telescope at Apache Point Observatory. The instrument is mounted at the Nasmyth focus, from which it receives an f/10 beam from the telescope. The slit plane holds either a $1'6 \times 1'6$ or a $1'6 \times 3'2$ slit. The main optics path is orthogonal to the local zenith, with the collimator fed by a folding flat just behind the slit. A Bausch and Lomb $31.6 \text{ line mm}^{-1}$ replica grating provides the high dispersion, and a pair of UBK7 prisms provides the cross-dispersion. The collimator defines an 8 inch beam which, after dispersion, feeds a 14 inch Schmidt camera. The detector is a Tektronix 2048×2048 CCD with $24 \mu\text{m}$ pixels.

The use of prismatic cross-dispersion allows efficient use of the CCD area so that complete spectral coverage is achieved from just shortward of 3400 Å to just longward of 10,200 Å. Each order is fully captured, so that a virtually blazeless echellogram can be obtained for each object by adding all redundant coverage of a given spectral interval. The resolving power is $37,500 (8 \text{ km s}^{-1})$, the read noise is 7 electrons pixel^{-1} , and the radiation rate is $0.013 \text{ pixel}^{-1} \text{ hr}^{-1}$. The half-peak counts are achieved at 4600 and 8200 Å for an unreddened F0 subdwarf star. The spectrograph

¹ Based on observations obtained with the Apache Point Observatory 3.5 m telescope, which is owned and operated by the Astrophysical Research Consortium.

design efficiency is 9% at $\lambda < 4100 \text{ \AA}$ and 3% at 3500 \AA . While we cannot confirm the efficiency until further tests are made on the telescope throughput, we believe that we are at or near the design goal. The instrument design principles of such spectrographs are given by Schroeder (1987), and the ARCES instrument is fully described by York et al. (2000).

The reddened stars HD 46711 and HD 50064 were chosen for their large color excesses, for their favorable placement in the late winter, and because it should be possible to observe H_2 in their spectra with the *Far-Ultraviolet Spectroscopic Explorer (FUSE)* ultraviolet spectrometer (Moos, Sembach, & Bianchi 1998). The star HD 183143 was observed because it is one of the stars used in the catalog of Jenniskens & Désert (1994) and because of its long history in the field (Herbig 1995). The star Cyg OB2 12 was selected because of its unusually large color excess and because the molecular ion H_3^+ has recently been observed in this source (McCall et al. 1998). The comparatively unreddened stars HD 164353 and HD 186994 were chosen because of their spectral types and favorable placement in the summer. We have not attempted telluric correction for any of the spectra, and any telluric interference can be judged from the spectra of these unreddened comparison stars.

Table 1 lists the stars and their spectral type and luminosity classes, V -band magnitudes, color excesses, stellar velocities with respect to the local standard of rest, stellar line widths, and interstellar LSR velocities and full widths. Also listed are the dates of observation and exposure times.

The data reduction started with the standard IRAF routines CCDPROC and DOECSLIT, which processed the CCD frames, extracted each order of the echelle, and (air) wavelength-calibrated the orders based on comparison exposures of a Th-Ar lamp. It was recently discovered that because of the large pixel scale of the CCD and the close spacing of the orders, the APTRACE routine introduces an unpredictable fringing (aliasing) into the spectra, which reduces the effective signal-to-noise ratio. Attempts are under way to modify the APTRACE procedure to prevent this effect, but they have not yet been successful. This

problem does not change our conclusions about the relatively sharp lines we have observed, but its resolution may enable the detection of weaker and broader lines in our data.

After each order was extracted and wavelength-calibrated by IRAF, it was transferred into IGOR PRO (version 3.14), a commercial graphing and analysis program produced by Wavemetrics. Within the IGOR environment, the orders were coadded in wavelength space to form a single array of data for each exposure. All exposures from a single night were then coadded, with small wavelength shifts used to align telluric absorption lines when necessary because of wavelength calibration errors.

The same extraction and coadding routine was performed on flat-field exposures of a tungsten filament housed in a quartz envelope. The large-scale spectral profile of each resulting flat-field spectrum was then removed by dividing out a 13th order polynomial fit to the spectrum. This afforded a normalized spectrum, which contained only information on pixel-to-pixel sensitivity variations. Each coadded stellar spectrum was then divided by this normalized flat field. In the case of HD 46711, the resulting flat-fielded spectra for each night were coadded after aligning the interstellar K I line at 7699 \AA . Finally, each flat-fielded spectrum was divided by a 13th order polynomial fit to provide a flat continuum for analysis.

3. RESULTS AND DISCUSSION

3.1. Laboratory Spectrum of C_7^-

The spectrum of C_7^- observed in the laboratory can be separated into two electronic transitions, the $A^2\Pi_u \leftarrow X^2\Pi_g$ system and the $B^2\Pi_u \leftarrow X^2\Pi_g$ system. The latter system lies to higher energy and is intrinsically broadened by internal conversion. While the intensities of the two systems are comparable, the large width of the $B \leftarrow X$ lines make their astronomical detection extremely difficult. All of the lines observed in the laboratory and expected in interstellar space originate in the ground vibrational level of the ground (X) electronic state.

TABLE 1
STELLAR DATA AND OBSERVING LOG

Star	Type ^a	V^a (mag)	E_{B-V}^b (mag)	v^{*c} (km s^{-1})	Δv^{*d} (km s^{-1})	v_{IS}^e (km s^{-1})	Δv_{IS}^e (km s^{-1})	UT Date (1999)	Integration Time (minutes)
Reddened Stars									
HD 46711	B3 II	9.1	1.05	23	84	8	19	Feb 01	30
								Feb 03	60
								Feb 07	50
								Feb 20	60
								Feb 22	60
HD 50064	B6 Ia	8.2	0.85	61	88	18	40	Feb 22	60
Cyg OB2 No. 12.....	B5 Iab	12.5	3.2	25	70	7	19	May 31	60
HD 183143	B7 Ia	6.9	1.28	34	69	7	23	Jun 10	35
Unreddened Stars									
HD 164353	B5 Ib	4.0	0.12	13	69	2	13	Jun 10	6
HD 186994	B0 III	7.5	0.19	-52	231	2	17	Jun 10	30

^a From the SIMBAD Astronomical Database.

^b From Snow, York, & Welty 1977.

^c Determined from He D₃ lines in our spectra.

^d FWHM of He I $\lambda 7065$.

^e Determined from K I $\lambda 7699$.

The $A \leftarrow X$ system consists of a progression of vibrational bands, starting with the origin band at 6270.2 Å, which is the strongest band and corresponds to transitions from the ground vibrational state of the X electronic state to the ground vibrational state of the A (first excited) electronic state. In all of the laboratory spectra obtained to date, the resolution is not sufficiently high to resolve the rotational structure of the bands.

In addition to the strong origin band, the $A \leftarrow X$ system shows a progression of weaker bands, which represent transitions into vibrationally excited states of the A electronic state. These transitions are described by the vibrational mode that is excited, the number of quanta of this mode in the lower state (always 0), and the number of quanta in the upper state. We utilize the standard notation introduced by J. K. G. Watson (Brand et al. 1983), in which, for example, 3_0^1 represents a transition into the state in the A electronic state where the ν_3 mode is singly excited. The bands reported by Tulej et al. (1998), in addition to the origin band (0_0^0), are 3_0^1 at 6064.0 Å, 2_0^1 at 5747.6 Å, 1_0^1 at 5612.8 Å, $1_0^1 3_0^1$ (a combination band, which happens to be a doublet) at 5456.7 and 5449.6 Å, 1_0^2 (also a doublet) at 5095.7 and 5089.5 Å, and $1_0^2 3_0^1$ at 4963.0 Å.

Because of the nature of the experimental technique, the intensities of the gas-phase lines obtained with the resonance-enhanced two-color photodetachment technique are unreliable as a result of power-broadening and saturation effects. Therefore, the intensities of the neon-matrix absorptions must be used in comparison with astronomical spectra. For this purpose, we have remeasured the relative intensities of the C_7^- bands from original spectra provided by J. P. Maier (1999, private communication), and these intensities are listed in Table 2. Because of contamination in the spectrum given by Forney et al. (1997), our intensities differ slightly from, and should be considered more accurate than, those listed in Tulej et al. (1998).

It should be emphasized that the C_7^- lines are just above the level of sensitivity of the gas-phase techniques. The diffi-

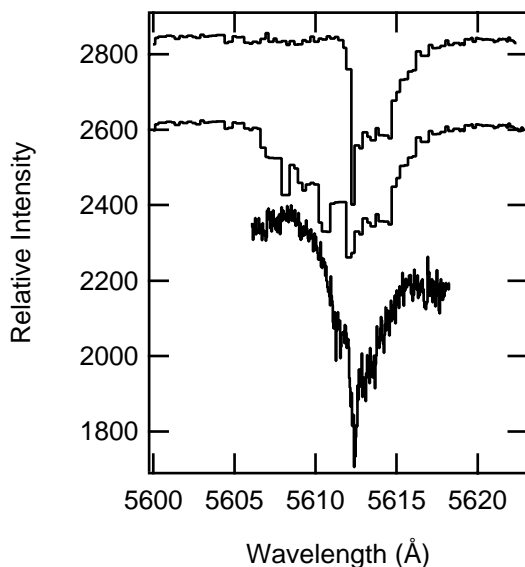


FIG. 1.—Top to bottom: Three traces of the 1_0^1 band of C_7^- from the gas-phase experiments of M. Tulej, M. Pachkov, and J. P. Maier (1999, private communication); trace from Tulej et al. (1998), trace from Fig. 5, and trace from a more recent experiment with higher instrumental resolution.

culties in the experiment are illustrated by the differences in the three traces provided by M. Tulej, M. Pachkov, and J. P. Maier (1999, private communication) in Figure 1. According to the experimenters, the width and shape of the absorption features are extremely dependent on experimental conditions, and one must not try to overinterpret the details of the spectra. The lack of repeatability in the current state-of-the-art laboratory measurements makes detailed comparisons with astronomical spectra challenging.

3.2. Diffuse Band Spectra

Spectra of the $\lambda 6270$ diffuse band, along with the laboratory trace of the C_7^- origin band, are shown in Figure 2. Also shown, for comparison, is a simulation of the diffuse-band catalog of Jenniskens & Désert (1994). This line (with FWHM ~ 1.2 Å) is clearly observed in all four reddened stars and is only slightly present in the “unreddened” [$E(B-V) = 0.12$] star HD 164353. There is good wavelength agreement between the astronomical lines and the sharp feature in the laboratory data.

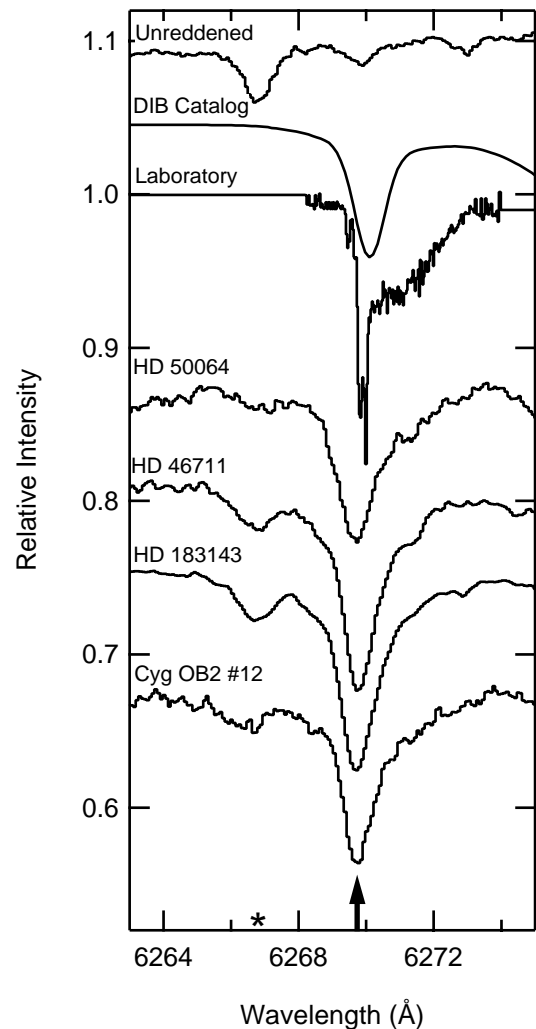


FIG. 2.—Origin (0_0^0) band of C_7^- and the diffuse band at 6270 Å attributed to it. Trace labeled “DIB catalog” is derived from the catalog of Jenniskens & Désert (1994). Stellar spectra have been shifted from unity for clarity and have been adjusted to rest air–wavelengths using the K I line at 7699 Å. The top trace is the (relatively) unreddened star HD 164353. The position of the diffuse band is marked with an arrow along the bottom axis, and the asterisk indicates a stellar line.

TABLE 2
LINE INTENSITIES

SOURCE	$\lambda 6270/0_0^0$		$\lambda 6065/3_0^1$		$\lambda 5610/1_0^1$		$\lambda 4964/1_0^2 3_0^1$	
	W_λ	$\sigma(W_\lambda)$	W_λ	$\sigma(W_\lambda)$	W_λ	$\sigma(W_\lambda)$	W_λ	$\sigma(W_\lambda)$
Laboratory	1	0.2	0.16	0.03	0.22	0.04	0.12 ^a	0.02
HD 50064	152	22	16	6	24	10	23 ^b	4
HD 46711	180	16	19	6	20	10	26 ^b	6
HD 183143	190	23	15	3	24	10	22	3
Cyg OB2 12.....	174	26	13	6	20	10	... ^c	...

NOTE.—Intensities for astronomical spectra are listed as equivalent widths W_λ in mÅ. Their uncertainties $\sigma(W_\lambda)$ are rough estimates based on the uncertain placement of the continuum. Laboratory (matrix) line intensities have been remeasured from the original spectra. They are in arbitrary units and have uncertainties of 20% (Tulej et al. 1998).

^a The $1_0^2 3_0^1$ line lies on the shoulder of the $0_0^0 B \leftarrow X$ transition, and thus it is difficult to estimate its intensity. The value listed should be considered a lower limit.

^b The equivalent width measurement of $\lambda 4964$ toward these sources is complicated by an instrumental artifact (seen in Fig. 4). The W_λ listed here were measured from the unflattened spectra, and corrections for the artifact have been attempted. This artifact did not affect HD 183143 because of the different Doppler shift.

^c The $\lambda 4964$ line was marginally detected toward Cyg OB2 12 but with a very low signal-to-noise ratio due to the high reddening of the object.

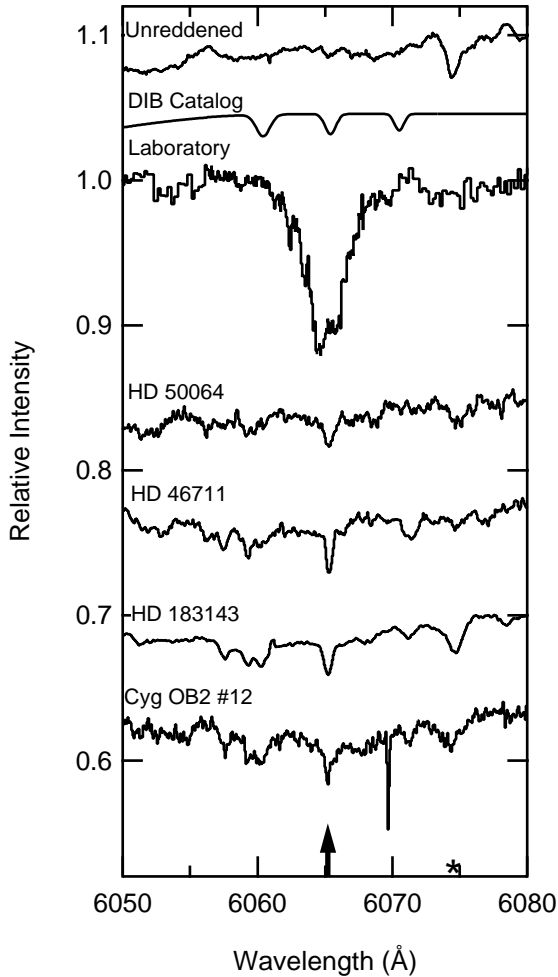


FIG. 3.—Same as Fig. 2, but for the 3_0^1 band of C_7^- and the diffuse band near 6065 Å. Note that the wavelength scale in this and the following figures is different from Fig. 2.

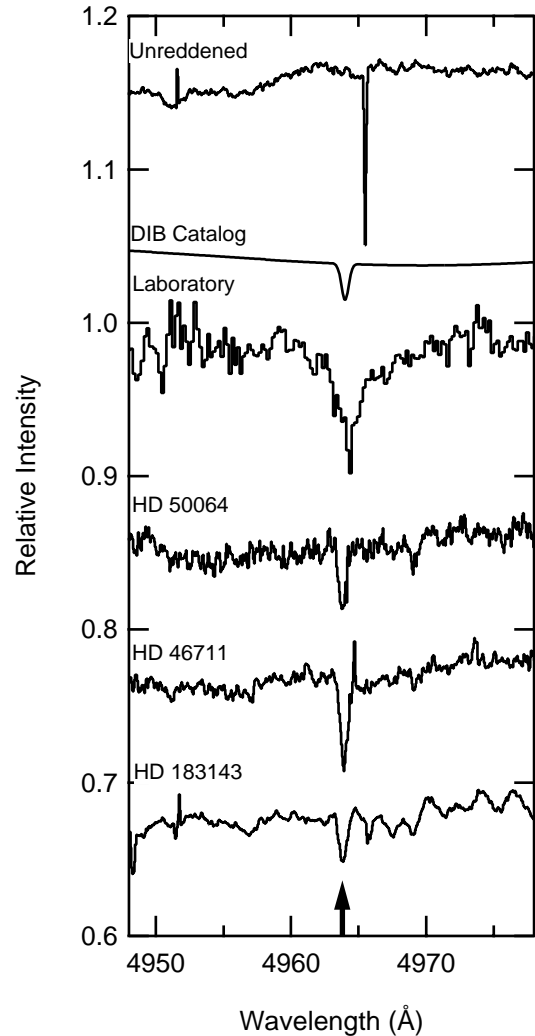


FIG. 4.—Same as Fig. 3, but for the $1_0^2 3_0^1$ band of C_7^- and the diffuse band near 4964 Å. Cyg OB2 12 is not shown because of its low signal-to-noise ratio at blue wavelengths.

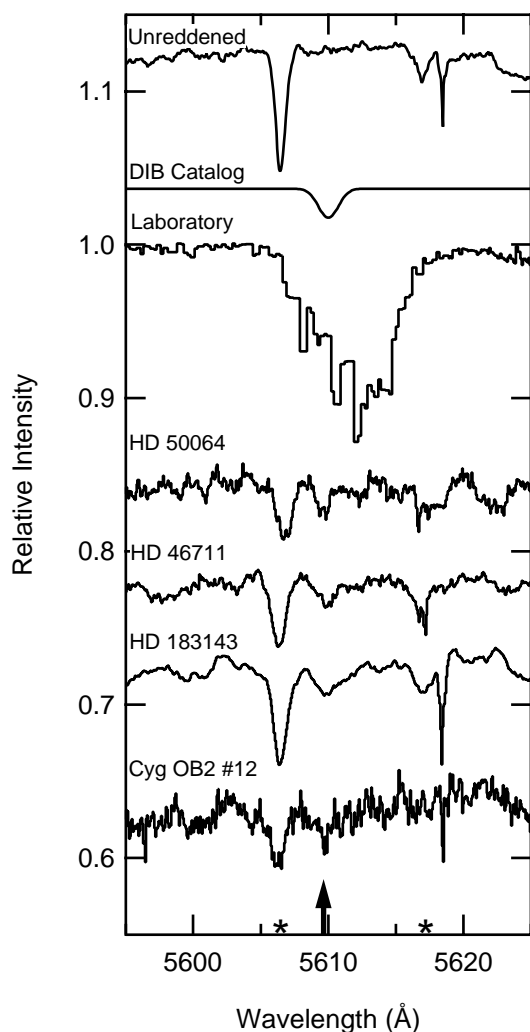


FIG. 5.—Same as Fig. 3, but for the 1_0^1 band of C_7^- and the diffuse band near 5610 Å.

Figure 3 shows the spectra of $\lambda 6065$, attributed to the C_7^- 3_0^1 band (note that the wavelength scale in this and the following figures differs from that of Fig. 2). The line is very sharp (FWHM ~ 0.7 Å), is present in all four reddened stars, and shows good wavelength agreement with the laboratory data. The two nearby “probable” diffuse bands of Jenniskens & Désert (1994) are difficult to pick out.

Figure 4 shows the diffuse band near 4964 Å, which is attributed to the $1_0^2 3_0^1$ combination band of C_7^- . This feature, like $\lambda 6065$, is quite sharp (FWHM ~ 0.7 Å) and clearly present in HD 50064, HD 46711, and HD 183143. The feature is also marginally present in Cyg OB2 12, which has very low flux at such blue wavelengths because of its extinction.

Figure 5 shows our spectra of the $\lambda 5610$ diffuse band, attributed to the 1_0^1 band of C_7^- . The astronomical line (FWHM ~ 1 Å) falls within the envelope of the laboratory data shown, but there is some uncertainty as to the intensity distribution of the laboratory line (see Fig. 1). The diffuse band is approximately 2 Å away from the maximum of the laboratory peak. This wavelength discrepancy must be explained or resolved by further experiments to conclusively assign this diffuse band to C_7^- .

Figure 6 shows the position of the 2_0^1 band of C_7^- , at 5747.6 Å. Jenniskens & Désert (1994) claim a “certain”

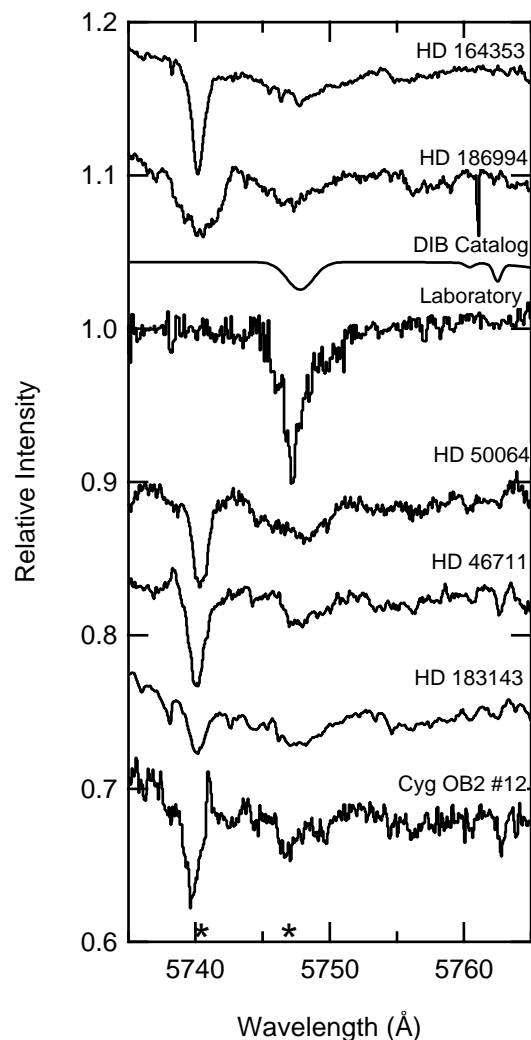


FIG. 6.—Same as Fig. 3, but for the 2_0^1 band of C_7^- . The spectra of the two unreddened stars HD 164353 and HD 186994 are very similar to those of the reddened stars near the position of the laboratory line, so it is difficult to confirm the presence (or absence) of a weak diffuse band corresponding to the 2_0^1 band.

diffuse band at 5747.8 Å, but their identification may be confused by the presence of stellar lines at this position. As is evident in Figure 6, the spectra of the unreddened stars HD 164353 and HD 186994 are very similar to those of the reddened stars at the position of the 2_0^1 band. Because of this, and the intrinsic weakness of the transition (its laboratory intensity is 0.05, compared with the origin band), it is difficult to confirm or refute the existence of a diffuse band at this position, which would correspond to the 2_0^1 C_7^- band.

The two doublets corresponding to the $1_0^1 3_0^1$ and 1_0^2 bands of C_7^- were not detected in the astronomical spectra. From the matrix spectra (in which the doublets are not resolved), we estimate total intensities of 0.04 and 0.09, respectively, for these two bands. Because of their low intensity, these bands are not detectable given the current signal-to-noise ratio of the observations.

Neither were the $B \leftarrow X$ bands of C_7^- detected. These bands are intrinsically broadened by internal conversion and have FWHM ~ 20 Å, about 20 times that of the $A \leftarrow X$ bands. Since the integrated laboratory intensity of the strongest $B \leftarrow X$ band is no greater than that of the $A \leftarrow X$

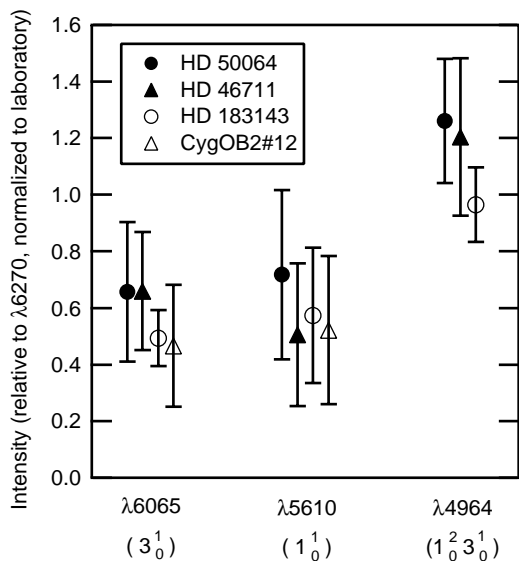


FIG. 7.—Equivalent widths of the diffuse bands attributed to C_7^- , relative to $\lambda 6270$ (the origin band), and normalized to the intensities of the laboratory matrix data. The error bars represent 1σ uncertainties as listed in Table 2.

origin band at 6270 \AA , these very broad lines will be difficult to detect in astronomical spectra. The present sensitivity and problems with flat-fielding completely exclude the possibility of detecting these bands in our spectra.

The equivalent widths of the observed diffuse bands, along with the estimated uncertainties, are listed in Table 2. If the four diffuse bands ($\lambda\lambda 6270, 6065, 5610,$ and 4964) are to be assigned to C_7^- , their relative intensities should remain constant from star to star, and should also agree with laboratory matrix data within the corresponding uncertainties. This agreement can be judged from Figure 7, in which the intensities of the three weaker bands relative to $\lambda 6270$, normalized to the matrix intensities, are plotted. Deviations of all data points for a particular band from unity would indicate disagreement with the laboratory matrix data, while scatter between the data points for a given band would indicate that the diffuse bands do not share a common carrier. Not accounted for in Figure 7 are the uncertainties in the equivalent widths of $\lambda 6270$, which could cause systematic shifts in the data points for an individual star (e.g., to lower all the closed circles). Given the uncertainties in the measurements, the intensity information does not seem to exclude the possibility that all four bands can be attributed to C_7^- .

The final consideration in comparing diffuse bands to the laboratory data is the line widths. Although it is difficult to accurately measure the line widths of the diffuse bands, they all have FWHM near $0.7\text{--}1.2 \text{ \AA}$. Because the temperature distribution is not well known in the laboratory experiments or in the astronomical sources and because the molecular constants (spin-orbit coupling and rotational constant in the ground and excited states) are unknown, it is quite possible that the interstellar line widths might be different from the laboratory line widths.

In the cases of the $1_0^1, 3_0^1,$ and $1_0^2 3_0^1$ bands, the astronomical line width is smaller than the laboratory line width, which poses no problem in the assignment. In the case of the origin band, however, there is an apparent discrepancy:

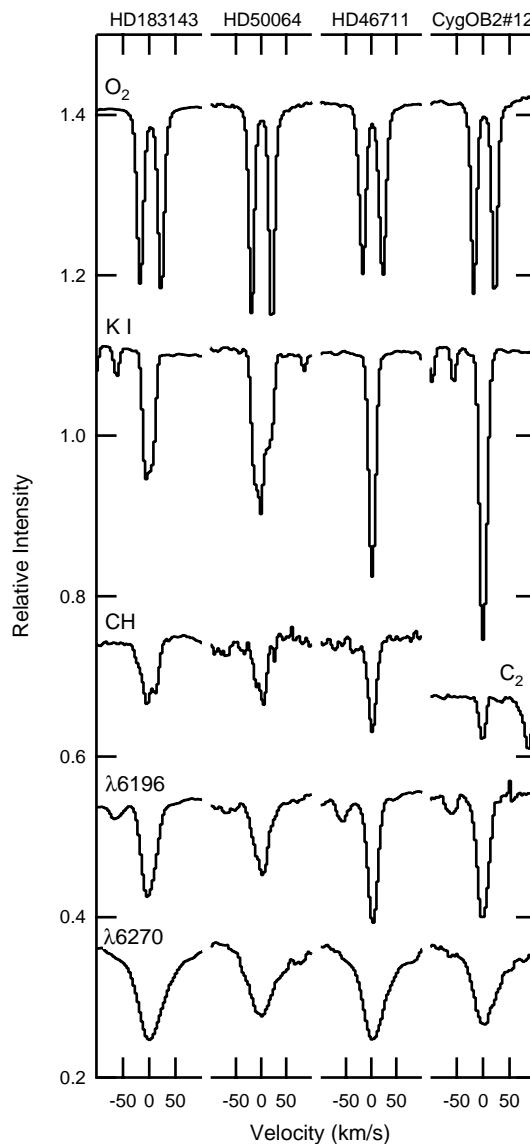


FIG. 8.—Profiles of telluric O_2 , interstellar $K I$, CH and C_2 , and the narrow diffuse band at 6196 \AA , compared with the $\lambda 6270$ diffuse band, attributed to the origin band of C_7^- . The $\lambda 6270$ band is clearly broader than can be explained by the velocity distribution of the atomic or molecular interstellar gas. The O_2 and $K I$ lines have been divided by 2 for clarity.

the profile of the $\lambda 6270$ diffuse band does not show the sharp peak (presumably the R -heads) that is present in the laboratory data (see Fig. 2). If the assignment to C_7^- is correct, this implies that either this sharp peak is not present at the temperature of the diffuse interstellar medium, or the peak has been “smeared out” by the velocity distribution of the gas.

Figure 8 demonstrates that the width of $\lambda 6270$ cannot be explained by the velocity distribution of either the atomic or molecular gas. The $\lambda 6270$ diffuse band in all four sources is significantly broader than the lines of $K I$, CH (in the cases of HD 46711, HD 50064, and HD 183143), C_2 (in Cyg OB2 12), and the narrow diffuse band $\lambda 6196$. The question of whether the observed profile of $\lambda 6270$ can be explained by temperature differences is key to the assignment of these diffuse bands to C_7^- and may remain unanswered until better laboratory data become available.

It is interesting to note from Tables 1 and 2 that the diffuse bands attributed to C₇⁻ do not behave linearly with reddening. Most notably, these bands are weaker in the spectrum of Cyg OB2 12 than in HD 183143, although the former star has more than twice the reddening. The relative deficiency of diffuse band strength per unit color excess toward Cyg OB2 12 has been known for some time (e.g., Bromage 1971; Wampler 1966). We plan to explore the relationships between various molecules by extending observations of H₃⁺ to stars of lower reddening (especially HD 183143) and extending observations of H₂ to higher reddenings (with *FUSE*), typically up to $E(B-V) \sim 1$.

4. CONCLUSIONS

Diffuse bands lying near four gas-phase laboratory bands of the C₇⁻ anion have been confirmed with high-resolution spectra of four highly reddened stars. The signal-to-noise ratio of the lines in these spectra is considerably better than in the diffuse-band catalog of Jenniskens & Désert (1994). The remaining laboratory lines of C₇⁻ are not expected to be detectable in our spectra because of stellar line confusion (2₀¹), their intrinsic weakness (1₀¹ 3₀¹ and 1₀²), or their intrinsic breadth (the $B \leftarrow X$ transitions).

The match in both wavelength and intensity is far better than has ever been attained by any proposed carrier; however, there remain two serious problems with the assignment of these four diffuse bands to C₇⁻. First, the diffuse band corresponding to 1₀¹ may be off by as much as 2 Å from the laboratory gas-phase data. Second, the profile of the λ6270 diffuse band differs substantially from that of the laboratory spectrum of the C₇⁻ origin band.

Better laboratory measurements are needed to confirm the wavelengths and intensity distributions of the C₇⁻ bands and, ideally, to resolve the bands rotationally. Rotational resolution would provide the information about the rotational constants and spin-orbit splitting necessary to predict the appearance of the spectrum at different tem-

peratures and would thus enable a more meaningful comparison with astronomical spectra. With this data in hand, it would be possible either to explain the apparent discrepancies between the laboratory and astronomical spectra or to state definitively that the discrepancies rule out the assignment of these diffuse bands to C₇⁻.

Further observational work may also be of assistance. Longer integration times and refinements in the flat-fielding procedure should lead to higher signal-to-noise ratios and may eventually enable an observational test of the presence or absence of the two doublets (1₀¹ 3₀¹ and 1₀²) of the $A \leftarrow X$ system or even of the very broad lines of the $B \leftarrow X$ system.

The probability of four lines accidentally showing such good wavelength and intensity agreement with diffuse bands is perhaps less than 1 in 10⁶, which strongly suggests that C₇⁻ is the carrier of these diffuse bands. However, the observed wavelength discrepancies and the profile of λ6270 are difficult to explain given our current understanding of the C₇⁻ molecule.

The referee has pointed out that Galazutdinov, Krelowski, & Musaev have also conducted diffuse-band observations specifically to check the possibility of C₇⁻ as a diffuse-band carrier and have reached a more pessimistic conclusion.

The authors wish to thank J. P. Maier, M. Tulej, and M. Pachkov for providing their laboratory data to enable a direct comparison with astronomical spectra; D. Duncan, L. M. Hobbs, C. Mallouris, and C. Rockosi for their assistance with the observations; and C. M. Lindsay and J. Thorburn for helpful discussions about data reduction and analysis. We are particularly grateful to R. Hildebrand for his extensive effort to deliver the echelle spectrograph in time for the 1999 January observing session. B. J. M. is supported by the Fannie and John Hertz Foundation. This work was supported by NSF grant PHYS-9722691 and NASA grant NAG5-4070.

REFERENCES

- Avery, L. W., Broten, N. W., Macleod, J. M., Oka, T., & Kroto, H. W. 1976, *ApJ*, 205, L173
 Brand, J. C. D., et al. 1983, *J. Mol. Spectrosc.*, 99, 482
 Bromage, G. E. 1971, *Nature*, 230, 172
 Douglas, A. E. 1977, *Nature*, 269, 130
 Forney, D., Grutter, M., Freivogel, P., & Maier, J. P. 1997, *J. Phys. Chem. A*, 101, 5292
 Herbig, G. H. 1995, *ARA&A*, 33, 19
 Jenniskens, P., & Désert, F.-X. 1994, *A&AS*, 106, 39
 McCall, B. J., Geballe, T. R., Hinkle, K. H., & Oka, T. 1998, *Science*, 279, 1910
 Moos, H. W., Sembach, K. R., & Bianchi, L. 1988, in *ASP Conf. Ser. 148, Origins*, ed. C. E. Woodward, J. M. Shull, & H. A. Thronson, Jr. (San Francisco: ASP), 304
 Ruffle, D. P., Bettens, R. P. A., Terzieva, R., & Herbst, E. 1999, *ApJ*, 523, 678
 Schroeder, D. J. 1987, *Astronomical Optics* (New York: Academic Press)
 Smith, W. H., Snow, T. P., Jr., & York, D. G. 1977, *ApJ*, 218, 124
 Snow, T. P., Jr., York, D. G., & Welty, D. E. 1977, *AJ*, 82, 113
 Tulej, M., Kirkwood, D. A., Pachkov, M., & Maier, J. P. 1998, *ApJ*, 506, L69
 Wampler, E. J. 1966, *ApJ*, 144, 921
 York, D. G., et al. 2000, in preparation